N73-24932
NASA CR-2266

NASA CONTRACTOR REPORT

NASA CR-2266

HEAT TRANSFER COEFFICIENTS OF DILUTE FLOWING GAS-SOLIDS SUSPENSIONS

by Ronald S. Kane and Robert Pfeffer

Prepared by
CITY UNIVERSITY OF NEW YORK
New York, N.Y. 10031
for Lewis Research Center

NATIONAL AERONAUTICS AND SPACE ADMINISTRATION • WASHINGTON, D. C. • JUNE 1973

1. Report No.	2. Government Accession No.	3. Recipient's Catalog No.
NASA CR-2266		

4. Title and Subtitle	5. Report Date
HEAT TRANSFER COEFFICIENTS OF DILUTE FLOWING GAS-SOLIDS SUSPENSIONS	June 1973
	6. Performing Organization Code

7. Author(s)	8. Performing Organization Report No.
Ronald S. Kane and Robert Pfeffer	None
	10. Work Unit No.

9. Performing Organization Name and Address	11. Contract or Grant No.
City University of New York New York, New York 10031	NGL 33-013-029

12. Sponsoring Agency Name and Address	13. Type of Report and Period Covered
National Aeronautics and Space Administration Washington, D.C. 20546	Contractor Report
	14. Sponsoring Agency Code

15. Supplementary Notes

Project Manager, Henry A. Putre, Nuclear Systems Division, NASA Lewis Research Center, Cleveland, Ohio

16. Abstract

Heat transfer coefficients of air-glass, argon-glass, and argon-aluminum suspensions were measured in horizontal and vertical tubes. The glass, 21.6 and 36.0 micron diameter particles, was suspended at gas Reynolds numbers between 11,000 and 21,000 and loading ratios between 0 and 2.5. The presence of particles generally reduced the heat transfer coefficient. The circulation of aluminum powder in the 0.870 inch diameter closed loop system produced tenacious deposits on protuberances into the stream. In the vertical test section, the Nusselt number reduction was attributed to viscous sublayer thickening; in the horizontal test section to particle deposition.

17. Key Words (Suggested by Author(s))		18. Distribution Statement
Deposition	Suspension	Unclassified - unlimited
Dilute	Turbulence	
Heat transfer	Viscous sublayer	
Pipe flow		

19. Security Classif. (of this report)	20. Security Classif. (of this page)	21. No. of Pages	22. Price*
Unclassified	Unclassified	31	$3.00

* For sale by the National Technical Information Service, Springfield, Virginia 22151

Table of Contents

Summary

The heat transfer coefficients of air-glass, argon-glass, and argon-aluminum suspensions were measured in horizontal and vertical 0.870 inch, inside diameter, tubes. Two grades of glass beads, averaging 21.6 microns and 36.0 microns diameter by weight, were suspended in the gas at gas Reynolds numbers between 11,000 and 21,000, at loading ratios between 0 and 2.5. The aluminum powder, averaging 30.0 microns diameter by weight, was suspended in the argon at argon Reynolds numbers between 11,000 and 21,000, at loading ratios between 0 and 1.0. The suspension was continuously recirculated in a closed loop system, originally designed for flow measurements but modified to permit heat transfer experiments.

The presence of particles generally reduced the heat transfer coefficients below those of the clean gas at corresponding gas flow rates. Reductions of up to 44% and 52% were achieved in the vertical test section for the 21.6 micron and 36.0 micron glass beads respectively. Reductions of up to 38% and 44% were also achieved in the horizontal test section for the 21.6 micron and 36.0 micron glass beads respectively. The exceptions to the general occurrence of Nusselt number reduction appeared either at low loading ratios or at low Reynolds numbers. The Nusselt number increases were always less than 20% and were usually less than 10%. With the exception of cases where deposition complicated the results, the suspension Nusselt numbers were independent of the carrying gas (air or argon) and were independent of particle properties (other than diameter).

The Nusselt number reduction in the vertical test section was considered as a coincident result of the drag reduction that had been observed earlier using the same experimental apparatus. The thickening of the viscous sublayer, the cause of the drag

reduction, was also believed to be the primary cause of the Nusselt number reduction. Visual observations of non-uniform particle concentration and of deposition in the horizontal test section indicated that the particles here took a more active role in the heat transfer mechanism. Therefore the Nusselt number reduction in the horizontal test section could not be attributed solely to the distortion of the fluid structure by the presence of particles. Thickening of the sublayer was probably more important in the vertical test section; and, particle deposition was probably more important in the horizontal test section.

The most unusual type of deposition was exhibited by the aluminum powder. Rock-hard deposits appeared on any protuberance into the flow channel. The aluminum powder welded itself to metallic objects by plastically deforming on collision with initial non-uniform deposits formed by other means. The other means of deposition, which were also appropriate to the glass beads, could have been caused by electrostatic attraction, gravity sedimentation, or thermophoresis.

Introduction

This report represents the final phase of a three phase investigation (ref. 1) into the existence, causes, and effects of drag and Nusselt number reduction. The first phase consisted of friction factor measurements which confirmed the existence of the gaseous drag reduction that was reported in an earlier study (refs. 2 - 3). The first phase also indicated that the behavior of a gas-solids suspension compared to that of the clean gas was a strong function of test section orientation, a moderate function of particle diameter, and a weak function of gas Reynolds number. The second phase of the investigation consisted of gas velocity,

gas turbulence intensity, gas turbulent spectra, and particle velocity profile measurements designed to elucidate the reasons for the drag reduction. These measurements (taken in a vertical test section) revealed that gaseous drag reduction could be characterized by thickening of the viscous sublayer in the presence of particles. The third phase of the investigation, reported here, consisted of heat transfer measurements with the aim of providing an analogy between drag reduction and Nusselt number reduction.

Previous investigators have reported decreased heat transfer when particles were added to a turbulent gaseous stream. A summary of earlier experimental evidence of Nusselt number reduction is shown in Table 1. Although experimental restrictions may have dictated the results, Nusselt number reduction has generally been limited to small particle sizes, small pipe diameters, low loading ratios, and low turbulent Reynolds numbers.

Only two of the investigators, Depew and Boothroyd, have measured both drag and Nusselt number reduction in the same test apparatus. However, neither Depew nor Boothroyd varied particle diameter, particle type, or test section orientation. In this phase of the investigation, three different particle diameters, two different particle types, and two different test section orientations were considered. The particles were two grades of glass beads, averaging 21.6 microns and 36.0 microns diameter by weight, and one grade of aluminum powder, averaging 30.0 microns diameter by weight. The test sections were vertical and horizontal 0.870 inch, inside diameter, tubes. The suspensions were circulated at gas (air or argon) Reynolds numbers between 11,000

Table 1

Experimental Evidence of Nusselt Number Reduction

Reference	Solids Diameter and Type	Pipe Diameter and Orientation	Loading Ratio	Reynolds Number
Farbar et al. 1957 (ref. 7)	10-210μ silica-alumina	0.69"vertical	0-0.20	13,500
			0-0.40	19,000
			0-0.70	23,000-27,000
Tien et al. 1962 (ref. 8)	30μ glass	0.71"vertical	0-2.5	15,000
			0-3.5	30,000
	30μ lead		0-3.0	15,000
			0-3.5	30,000
	200μ glass		0-3.5	15,000
			0-3.5	30,000
	200μ lead		0-3.5	15,000
			0-3.5	30,000
Abel et al. 1963 (ref. 9)	1-10μ graphite	0.89"vertical	0-5.0	22,000-65,000
Depew et al. 1963 (ref. 10)	30μ glass	0.71"vertical	0.5-3.0	13,500
			0.5-3.0	27,400
Farbar et al. 1963 (ref. 11)	30μ glass	0.67"vertical	0-1.5	15,300
			0-1.7	26,500
	70μ glass		2-3.0	15,300
Jepson et al. 1963 (ref. 12)	211-295μ sand	1.5"vertical	0-2.0	14,300
			0-4.0	21,450
			0-6.0	28,600
			0-11.0	42,900
	76-104μ sand		0-5.1	14,300-28,600
	422-599μ sand		0-10.1	28,600-71,500

Table 1 (cont.)

Reference	Solids Diameter and Type	Pipe Diameter and Orientation	Loading Ratio	Reynolds Number
Jepson et al. 1963 (ref. 12) (cont.)	850-1200μ sand	1.5"vertical	0-2.5	21,450-71,500
	1200-1680μ millet seed		0-8.5	21,450-71,500
Garret 1964 (ref. 13)	243μ sand	3"vertical	0-3.75	23,000
	159μ sand		0-5.5	30,700
Szekely et al. 1966 (ref. 14)	150, 300, 600, 1200μ sand 200μ bronze 175μ iron	cyclone	0-3.0	-----
Sukomel et al. 1967 (ref. 15)	65μ graphite	0.30"horizontal	0-8.0	15,000
Boothroyd et al. 1970 (ref. 16)	0-40μ zinc	1"vertical	0-20.	35,000
			0-8.0	53,000
			0-8.0	80,000
			0-5.0	100,000
		2"vertical	0-3.5	35,000
			0-3.0	53,000
			0-4.0	80,000
			0-2.5	100,000
		3"vertical	0-2.0	35,000
			0-2.0	53,000
			0-3.5	80,000
Depew et al. 1970 (ref. 17)	30μ glass	0.71"horizontal	0-4.5	10,000
			0-7.5	15,000
			0-4.0	30,000
	200μ glass		0-6.0	15,000
			0-5.0	30,000

and 21,000 and at loading ratios between 0 and 2.5.

The range of parameters chosen here for the heat transfer work was identical to the range of parameters considered earlier during pressure drop work with a few exceptions. During pressure drop measurements, 15.0 and 55.0 micron diameter glass beads were also considered. However, the 15.0 micron diameter glass beads were found to be extremely difficult to circulate as their small size permitted rapid deposition and plating on the walls of the closed loop. The 55.0 micron diameter glass beads were found to degrade after prolonged passage through the pump used to circulate the suspension in a closed loop operation. The 15.0 and 55.0 micron diameter glass beads would therefore not provide meaningful information after the long warmup periods required for heat transfer measurements.

The aluminum powder, not used during pressure drop measurements, was selected for heat transfer tests because it had different thermal properties from the glass beads and might give additional information on the heat transfer mechanism. Argon, also not used during pressure drop measurements, was chosen as the conveying medium for circulation of aluminum powder, because it would eliminate any possible hazard in the closed loop system by the buildup and release of static electric charges.

Experimental Apparatus and Procedures

The suspension was circulated through a closed loop system, originally designed for pressure drop and flow measurements but modified for heat transfer measurements. The closed loop system as modified for heat transfer is shown in Figure 1. The loop could have been described as a 12 foot high, 18½ foot long rectangle generally constructed of 1 inch outside diameter (O.D.),

0.065 inch wall, type 304 stainless steel tubing. The motive force for flow was provided by a centrifugal circulator which was capable of pumping gas and solids simultaneously.

Two primary test sections were provided, a heated vertical section and a cooled horizontal section. The vertical test section was fabricated from a 30 inch length of 1 inch O.D., 0.065 inch wall stainless steel tubing and located 92 tube diameters upstream of the nearest flow disturbance, the reinforced elbow near the circulator outlet. Miniature chromel-alumel thermocouples were located at either end of the test section and positioned to measure centerline bulk temperature. The thermocouples were inserted through mounting bushings welded to the tube wall. The bushings seated securely on the 1/16 inch O.D. thermocouple sheath and did not permit leakage. Two diametrally opposed chromel-alumel thermocouple junctions were located every six inches along the test section to measure outside wall temperatures.

The heat input in the vertical test section was supplied by an electrical resistance tape wrapped around the tube. The tape was controlled by a 0 to 120 volt range voltage regulator and supplied a maximum of 384 watts. Several inches of fiberglass and asbestos wool insulation were wrapped around the tape to minimize heat conduction to the atmosphere. A final layer of aluminum foil was added to minimize radiative heat losses.

A 48 inch long, 2 inch O.D., copper, water cooling jacket was located 78 inches downstream of the first reinforced elbow and served to identify the horizontal test section for heat transfer. Chromel-alumel bulk thermocouples were located at either end of the test section to measure suspension temperatures. ASTM A9F thermometers, reading to $1^{o}F$, were inserted through nylon fittings in the water jacket to measure the inlet and outlet water

temperatures. Another 48 inch long, 2 inch O.D., copper, water cooling jacket was located 72 inches from the unreinforced elbow in the lower horizontal section. Although this section was equipped with the same instrumentation as the upper horizontal section and was occasionally used as a test section, its main purpose was to protect the pump from excessive fluid temperatures. Five chromel-alumel thermocouples on the circulator were used to monitor housing and bearing temperatures. All thermocouple readings were taken from a 24 point dial recorder. The dial read to $5^{\circ}F$ over an $800^{\circ}F$ range but could be estimated to $1^{\circ}F$.

The gas flow rate was measured with a sharp-edged orifice even with particles in suspension. Earlier studies (refs. 1-3) had shown that the calibration of an orifice was unaffected by dilute volumetric concentrations of solids suspended in the gas. The solids flow rate was determined with the aid of a cantilevered target meter. The operation of the meter was based on the fact that the deflection of the cantilever (determined by strain gauges) was directly proportional to the force of the fluid impinging on the target. The force of the gas alone was known from the flow rate given by the sharp-edged orifice. The force of the solids was related to the solids flow rate. During calibration of the target-meter, the solids flow was determined directly in an open loop operation and used to separate the response of the target-meter to solids from the response of the target-meter to gas alone. Once the separate responses of the target-meter to the various particle sizes and to the gas was known, the target-meter was used to calculate the loading ratio in closed loop operation. The detailed calibration of this device will not be given here as it is lengthy and is described elsewhere (ref. 1).

Solids were added to the loop before a set of data runs by

pouring a given weight of sifted particles into the solids inlet port located near the circulator intake. The port was sealed and the circulator was started to disperse the particles through the loop. Not less than a one-hour warmup period with the circulator running preceded each set of heat transfer runs with a given amount of particles in the loop. The cooling water temperature and the maximum wall temperature in the vertical test section had to stabilize before reliable data could be taken. At the beginning of each set of data runs, the cooling water flow rate (monitored on a 0 to 1 gallon-per-minute rotameter reading to 0.02 gpm), the circulator shaft speed, and the voltage regulator setting were set to the desired values. Because of the limitations on the allowable tape temperature, the voltage regulator setting was adjusted so that the maximum wall temperature in the vertical test section did not exceed 420^{o}F. Although a one-hour warmup was required between sets of runs, only a fifteen minute period was required between individual runs where only the gas Reynolds number and not the amount of solids in the loop was varied. For argon gas measurements, the system was purged of air by forcing the denser argon into the lower loop and venting the lighter air from the upper loop. Additional details of the experimental apparatus and procedure are described in reference 1.

Clean Gas Test Results

Prior to suspension tests, heat transfer measurements were used to calculate the Nusselt numbers for the two gases, air and argon. The direction and instrumentation of the heat transfer was different for the vertical and horizontal test sections. Two different techniques were therefore used to calculate the gas side heat transfer coefficient and Nusselt number.

In the vertical test section, the heat input was calculated from:

$$Q = W_g C_{pg} (T_{OUT} - T_{IN}) \tag{1}$$

The heat input was equated to: $Q = UA(\bar{T}_W - \bar{T}_B)$ (2)

where $\bar{T}_W$ was an average wall temperature weighted in accordance with the linear spacing of the 12 thermocouples along the heated section with UA given by:

$$UA = \frac{1}{\frac{t_{ss}}{k_{ss}\bar{A}} + \frac{1}{h_i A_i}} \tag{3}$$

With the heat input and all the temperatures as known quantities, the gas side heat transfer coefficient was calculated directly.

In the horizontal test section, a counterflow heat exchanger equation was used to evaluate UA. The gas side heat loss was calculated from:

$$Q = W_g C_{pg} (T_{IN} - T_{OUT}) \tag{4}$$

The heat loss was equated to:

$$Q = UALMTD \quad \text{where} \quad LMTD = \frac{(T_{OUT} - T_{WOUT}) - (T_{IN} - T_{WIN})}{Ln\left(\frac{T_{OUT} - T_{WOUT}}{T_{IN} - T_{WIN}}\right)}$$

and

$$UA = \frac{1}{\frac{t_{ss}}{k_{ss}\bar{A}} + \frac{1}{h_o A_o} + \frac{1}{h_i A_i}} \tag{5}$$

In operation, the water temperature remained almost constant from the inlet to the outlet of the cooling jacket. The logarithmic temperature difference was almost exclusively dependent on variations in the gas temperature. The water flow rate was high enough that UA was sensitive only to the gas side coefficient. The

resistance of the stainless steel tube wall was negligible in both test sections.

The Nusselt number was evaluated at the average bulk gas temperature. The results for air and argon are shown in Figure 2 where Nusselt number is plotted versus Reynolds number. The measured Nusselt numbers were about 10 percent lower than the Nusselt numbers calculated from the Sieder-Tate equation which correlates experimental data within wide 30% limits (ref. 4). Prandtl number dependence was not an important factor because the one-third power of the Prandtl number for air and argon is essentially constant for the experimental range of temperatures. The clean gas values were the same in both the vertical and horizontal test sections and the lower horizontal cooling section as well. Clean gas Nusselt numbers were measured before and after suspension tests and were found to be unchanged.

Suspension Test Results and Discussion

The suspension heat transfer measurements were used to calculate Nusselt numbers for the two gases carrying suspended glass beads or aluminum powder. The circulation of suspensions required revision of the clean gas formulae for heat input in the vertical test section and heat loss in the horizontal test section. The mass flow rate now included the contribution of the suspended solids:

$$W_s = W_g(1 + \eta) \tag{6}$$

The specific heat of the suspension was calculated from a weighted average of the separate gas and solids specific heats:

$$c_{ps} = c_{pg} \frac{1 + \delta\eta}{1 + \eta} \tag{7}$$

where

$$\delta = \frac{c_{pp}}{c_{pg}}$$

The final calculations and correlations of Nusselt numbers were based on the gas properties (density, thermal conductivity, specific heats, and viscosity) in order to provide a direct comparison with the clean gas results. For the loading ratios of this study, the assumption that the effective thermal conductivity of the suspension was the same as the gas thermal conductivity introduced negligible error (ref. 5).

The results of the vertical test section heat transfer measurements are shown in Figure 3 for suspensions of the 21.6 micron glass beads in air and in Figure 4 for suspensions of the 36.0 micron glass beads in air and argon and suspensions of 30.0 micron aluminum powder in argon. The graphs were plotted as the ratio of the suspension Nusselt number to the clean gas Nusselt number versus loading ratio at corresponding gas Reynolds numbers. Nusselt number reduction was indicated by values of the Nusselt number ratio below unity. Figure 4 shows the envelope of the actual data. The upper limit generally represented the argon-glass results. The lower limit generally represented the air-glass and argon aluminum results.

The glass-air suspension measurements indicated that the 21.6 and 36.0 micron glass beads were much more effective in reducing Nusselt numbers than in reducing friction factors (ref. 1). Reductions of up to 44% and 52% were achieved in the vertical test

section for the 21.6 and 36.0 micron glass beads respectively. Like the friction factor results, there was a minimum loading ratio for the onset of Nusselt number reduction. Also like the friction factor results, the onset of Nusselt number reduction was further delayed with increased particle size. Neither of the two glass bead suspensions showed any Reynolds number effect on the onset of Nusselt number reduction or on the amount of Nusselt number reduction.

The suspensions of 21.6 micron glass beads showed a monotonic decrease in Nusselt number ratio after the onset of Nusselt number reduction. Before the onset of Nusselt number reduction at a loading ratio of 0.12, a moderate increase in Nusselt number was noted. The increase was attributed to an initial widely dispersed deposit on the test section wall. The deposit was apparently insufficient to cover large heat transfer areas but was sufficient to disturb the viscous sublayer, producing additional turbulence and heat transfer.

The suspensions of 36.0 micron glass beads in air showed a tendency toward a flat minimum at a loading ratio of 1.2. Before the onset of Nusselt number reduction at a loading ratio of 0.4, a slight increase in Nusselt number was noted. The increase was also attributed to a widely dispersed deposit on the vertical test section wall. That the increase was smaller for the 36.0 micron glass beads than for the 21.6 micron glass beads was consistent with the relative ability of the two bead sizes to plate out. For both bead sizes, the deposit, rather than accumulating further, was probably worn away by heavier loadings and did not affect the vertical test section results past the onset of Nusselt number reduction.

The measurements of Nusselt numbers for suspensions of the

36.0 micron glass beads in argon were performed in order to determine the effect of different gas properties on the Nusselt number reduction. The argon appeared to delay the onset of Nusselt number reduction to a loading ratio of 0.6 compared to 0.4 for air. However, the maximum amount of Nusselt number reduction was approximately the same for both gases. The general shape of the Nusselt number ratio versus loading ratio curves was also the same for both gases. These results were not surprising since the Prandtl numbers of air and argon were similar in the working temperature range.

The heat transfer measurements for suspensions of aluminum powder in argon indicated that particle thermal properties had no effect on Nusselt number reduction in the vertical test section. The 30.0 micron aluminum powder gave similar results as the 36.0 micron glass beads. The similarity in behavior of the two different particles in the vertical test section suggested that the Nusselt number reduction was a coincidental result of the drag reduction mechanism; that is, a thickening of the viscous sublayer.

The results of the horizontal test section heat transfer measurements are shown in Figure 5 for suspensions of the 21.6 micron glass beads in air and in Figure 6 for suspensions of the 36.0 micron glass beads in air and argon and suspensions of 30.0 micron aluminum powder in argon. Significant Nusselt number reduction, up to 38% and 44% for the 21.6 and 36.0 micron glass beads in air respectively, was also achieved for the horizontal test section. However, the horizontal test section Nusselt number results were not as consistent with the friction factor results as those in the vertical test section (ref. 1). (In the vertical

test section Nusselt number reduction occurred under the same conditions as the previously observed drag reduction. In the horizontal test section, Nusselt number reduction occurred even for those cases where drag increases and not drag reduction were previously observed.) Gravity sedimentation and thermophoresis causing deposition on the cool wall of the horizontal heat transfer test section apparently complicated the results.

The 21.6 micron glass beads (like the previous friction factor results) showed very similar results in both horizontal and vertical test sections with the exception of a detectable Reynolds number effect in the horizontal test section. The amount of Nusselt number reduction progressively decreased with decreasing Reynolds number. The onset of Nusselt number reduction was progressively delayed, from loading ratios of 0.07 to 0.16, with decreasing Reynolds numbers until the lowest Reynolds numbers, about 12,000 were reached. At Reynolds numbers of about 12,000, Nusselt number reduction was not generally noted. The observed loss of entrainment at these Reynolds numbers could presumably explain the anomalous results as the presence of large quantities of solids in direct contact with the tube wall would drastically change the heat transfer mechanism. With the exception of the low Reynolds number results, the trends of the heat transfer measurements for the 21.6 micron glass beads were reasonably consistent with the trends of the previous pressure drop measurements. However, it could not be concluded that the controlling mechanism in the horizontal test section was the same for both cases. Thickening of the sublayer was probably more important for the pressure drop measurements; and, particle deposition was probably more important for the heat transfer measurements.

The results for suspensions of 36.0 micron glass beads in air

were less predictable and systematic than the results for the 21.6 micron glass beads. Whereas, friction factor increases were previously noted at all test conditions for the 36.0 micron glass beads (ref. 1), Nusselt number increases were found only for the loading ratios less than 0.4 or for Reynolds numbers of about 12,000. In general, substantial Nusselt number decreases were observed. The friction factor and heat transfer results for the 36.0 micron glass beads tended to confirm the conjecture that particle deposition was more important for the Nusselt number reduction in the horizontal test section than any uniform sublayer changes. The onset and amount of Nusselt number reduction did not follow the consistent pattern observed with tests of 21.6 micron glass bead suspensions. It was apparent that the Reynolds analogy which predicts corresponding effects on heat transfer and momentum transfer was not valid for horizontal flow. The particles did not just distort the structure of the turbulence as they did in vertical flow, but actually became an active part of the heat transfer mechanism.

The data obtained with suspensions of 36.0 micron glass beads in argon were in agreement with the air suspension data. However, the aluminum-argon suspension data always indicated Nusselt number increases regardless of loading ratio or Reynolds number. These results were probably caused by deposition of the powder on the cool wall of the horizontal test section. The unusual nature of the aluminum deposits probably disturbed the flow pattern and produced additional turbulence. Reductions in local heat transfer rates directly at the deposit locations were probably quite small because of the high thermal conductivity of the aluminum. Therefore, it was likely that the additional turbulence, aiding heat

transfer, more than offset the local fouling factors, hindering heat transfer.

The form of the aluminum deposit was quite unusual, especially on protuberances into the flow channel. A rock-hard build-up of aluminum was observed on any surface subject to direct bombardment. Very heavy accumulations were noted on thermocouples, the target meter, and the internals of the circulator. Figure 7 shows the type of deposit that was found on all thermocouples after bombardment by aluminum powder.

The propensity of the aluminum powder to bond so solidly to the loop walls and equipment may have been the result of its wide size distribution. Although the aluminum powder averaged 30.0 microns diameter by weight, the powder included particle sizes ranging from 5.8 to 55.0 microns diameter. Boothroyd (ref. 6) maintains that a polydisperse powder will afford a much greater number of additional cohesive contact points than a narrowly sized powder (like the glass beads). The aluminum powder welded itself to metallic objects by plastically deforming on collision with initial non-uniform deposits formed by other means. The other means of deposition could have been caused by electrostatic attraction, gravity sedimentation, or thermophoresis.

Conclusions

The heat transfer coefficients of air-glass, argon-glass, and argon-aluminum suspensions were measured in horizontal and vertical tubes. The results of these tests led to the following conclusions:

1. The presence of dilute loadings of small particles in a turbulent stream reduced the heat transfer coefficient below

that of the clean gas at corresponding gas flow rates. Reductions of up to 44% and 52% were achieved in the vertical test section for 21.6 and 36.0 micron diameter glass beads respectively. Reductions of up to 38% and 44% were also achieved for the horizontal test section.

2. The Nusselt number reduction in the vertical test section was attributed to a postulated drag reduction mechanism observed previously under the same experimental conditions; that is, thickening of the viscous sublayer. This conclusion was based on the fact that heat transfer measurements with suspensions of aluminum powder in argon showed that particle thermal properties had no effect on Nusselt number reduction in the vertical test section.
3. Gravity segregation and thermophoresis causing deposition on the cool wall of the test section complicated the results in the horizontal test section. The Reynolds analogy was not considered valid for horizontal flow because the particles did not just distort the structure of the turbulent fluid, as they did in vertical flow, but actually became an active part of the heat transfer mechanism.
4. The aluminum powder produced unusual deposits. Rock-hard deposits appeared on any protuberance into the flow channel. The aluminum welded itself to metallic objects by plastically deforming on collision with initial non-uniform deposits formed by other means. The other means of deposition could have been caused by electrostatic attraction, gravity sedimentation, or thermophoresis.

List of Symbols

A	heat transfer surface area in equations 2, 3, and 5, ft^2.
A_i	inside heat transfer surface area, ft^2.
A_o	outside heat transfer surface area, ft^2.
$\bar{A}$	average heat transfer surface area for conduction, ft^2.
C_{pg}	specific heat capacity of gas, $Btulbm^{-1}F^{-1}$.
C_{pp}	specific heat capacity of a particle, $Btulbm^{-1}F^{-1}$.
C_{ps}	specific heat capacity of suspension, $Btulbm^{-1}F^{-1}$.
D	pipe inside diameter, ft.
h_i	inside heat transfer coefficient, $Btuhr^{-1}ft^{-2}F^{-1}$.
h_o	outside heat transfer coefficient, $Btuhr^{-1}ft^{-2}F^{-1}$.
k_g	gas thermal conductivity, $Btuhr^{-1}ft^{-1}F^{-1}$.
k_{ss}	stainless steel thermal conductivity, $Btuhr^{-1}ft^{-1}F^{-1}$.
LMTD	logarithmic mean temperature difference, F.
Nu_g	$h_i D k_g^{-1}$, Nusselt number in clean gas flow, dimensionless.
Nu_s	$h_i D k_g^{-1}$, Nusselt number in suspension flow, dimensionless.
Pr	$C_{pg}\ \mu k_g^{-1}$; Prandtl number of gas, dimensionless.
Q	heat transferred, $Btuhr^{-1}$.
Re_g	$UD\nu^{-1}$, Reynolds number based upon gas properties, dimensionless.
t_{ss}	thickness of stainless steel tube wall, ft.
T_g	gas temperature, F.
T_{IN}	inlet suspension temperature, F.
T_{OUT}	outlet suspension temperature, F.
T_{WIN}	inlet water temperature, F.

T_{WOUT} outlet water temperature, F.

$\bar{T}_B$ average of inlet and outlet suspension temperatures, F.

$\bar{T}_W$ weighted average of wall temperatures in vertical test section, F.

U bulk average gas velocity in definition of Reynolds number, $\bar{U}$ ftsec^{-1}.

U overall heat transfer coefficient, Btuhr^{-1}ft^{2}F^{-1}.

W_g mass flow rate of gas only, lbmsec^{-1} or lbmhr^{-1}.

W_p mass flow rate of particles only, lbmsec^{-1} or lbmhr^{-1}.

W_s mass flow rate of suspension, lbmsec^{-1} or lbmhr^{-1}.

δ ratio of specific heat of particle to specific heat of gas, dimensionless.

η $W_p W_g^{-1}$, loading ratio, dimensionless.

μ gas viscosity, lbmft^{-1}sec^{-1}.

ν gas kinematic viscosity, ft^{2}sec^{-1}.

References

1 Kane, R.S. 1973. Drag reduction in dilute flowing gas-solids suspensions. Ph.D. Thesis, City University of New York.

2 Rossetti, S.J. 1969. Experimental determination of pressure drop and flow characteristics of dilute gas-solid suspensions. Ph.D. Thesis, City University of New York.

3 Pfeffer, R. and Rossetti, S.J. 1971. Experimental determination of pressure drop and flow characteristics of dilute gas-solid suspensions. NASA CR-1894.

4 Kreith, F. 1964. Principles of Heat Transfer. Scranton: International Textbook Co.

5 Pfeffer, R., Rossetti, S., and Lieblein, S. 1966. Analysis and correlation of heat transfer coefficient and friction factor data for dilute gas-solid suspensions. NASA TN D-3603.

6 Boothroyd, R.G. 1971. Flowing Gas-Solids Suspensions. London: Chapman and Hall Ltd.

7 Farbar, L. and Morley, M.J. 1957. Heat transfer to flowing gas-solids mixtures in a circular tube. Ind. Eng. Chem., 49, 1143-1150.

8 Tien, C.L. and Quan, V. 1962. Local heat transfer characteristics of air-glass and air-lead mixtures in turbulent pipe flow. ASME Paper 62-HT-15.

9 Abel, W.T., Bluman, D.E., and O'Leary, J.P. 1963. Gas-solids suspensions as heat-carrying mediums. ASME Paper 63-WA-210.

10 Depew, C.A. and Farbar, L. 1963. Heat transfer to pneumatically conveyed glass particles of fixed size. Trans. ASME, J. Heat Transfer, 85, 164-172.

11 Farbar, L. and Depew, C.A. 1963. Heat transfer effects to gas-solids mixtures using solid spherical particles of uniform size. Ind. Eng. Chem. Fundamentals, 2, 130-135.

12 Jepson, G., Poll, A., and Smith, W. 1963. Heat transfer from gas to wall in a gas/solids transport line. Trans. Instn. Chem. Engrs., 41, 207-211.

13 Garrett, T. 1964. Heat transfer characteristics of dilute phase solids-air suspensions in turbulent pipe flow. Ph.D. Thesis, Dep. of Engg., Cambridge University, England.

14 Szekely, J. and Carr, R. 1966. Heat transfer in a cyclone. Chem. Eng. Sci., 21, 1119-1132.

15 Śukomel, A.S., Tsvetkov, F.F., and Kerimov, R.V. 1967. A study of local heat transfer coefficients from a tube wall to a turbulent flow of gas bearing suspended solid particles. Teploenergetika, 14, 77-80. App. Mech. Rev. 1968, 21, 6834.

16 Boothroyd, R.G. and Haque, H. 1970. Fully developed heat transfer to a gaseous suspension of particles flowing turbulently in ducts of different size. J. Mech. Eng. Sci., 12, 191-200.

17 Depew, C.A. and Cramer, E.R. 1970. Heat transfer to horizontal gas-solid suspension flows. Trans. ASME, J. Heat Transfer, 92, 77-82.

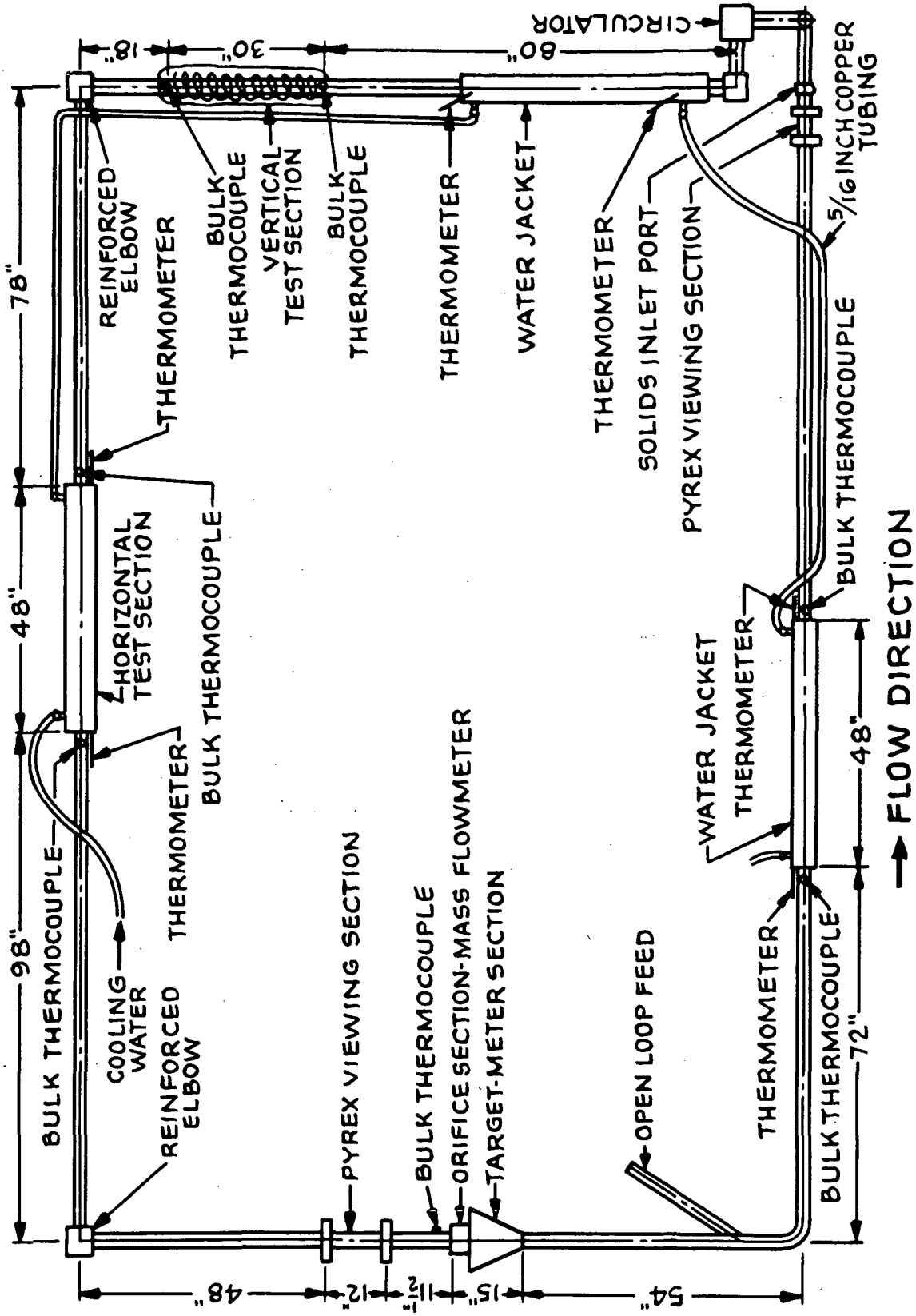

Figure 1

Closed Loop Modified for Heat Transfer

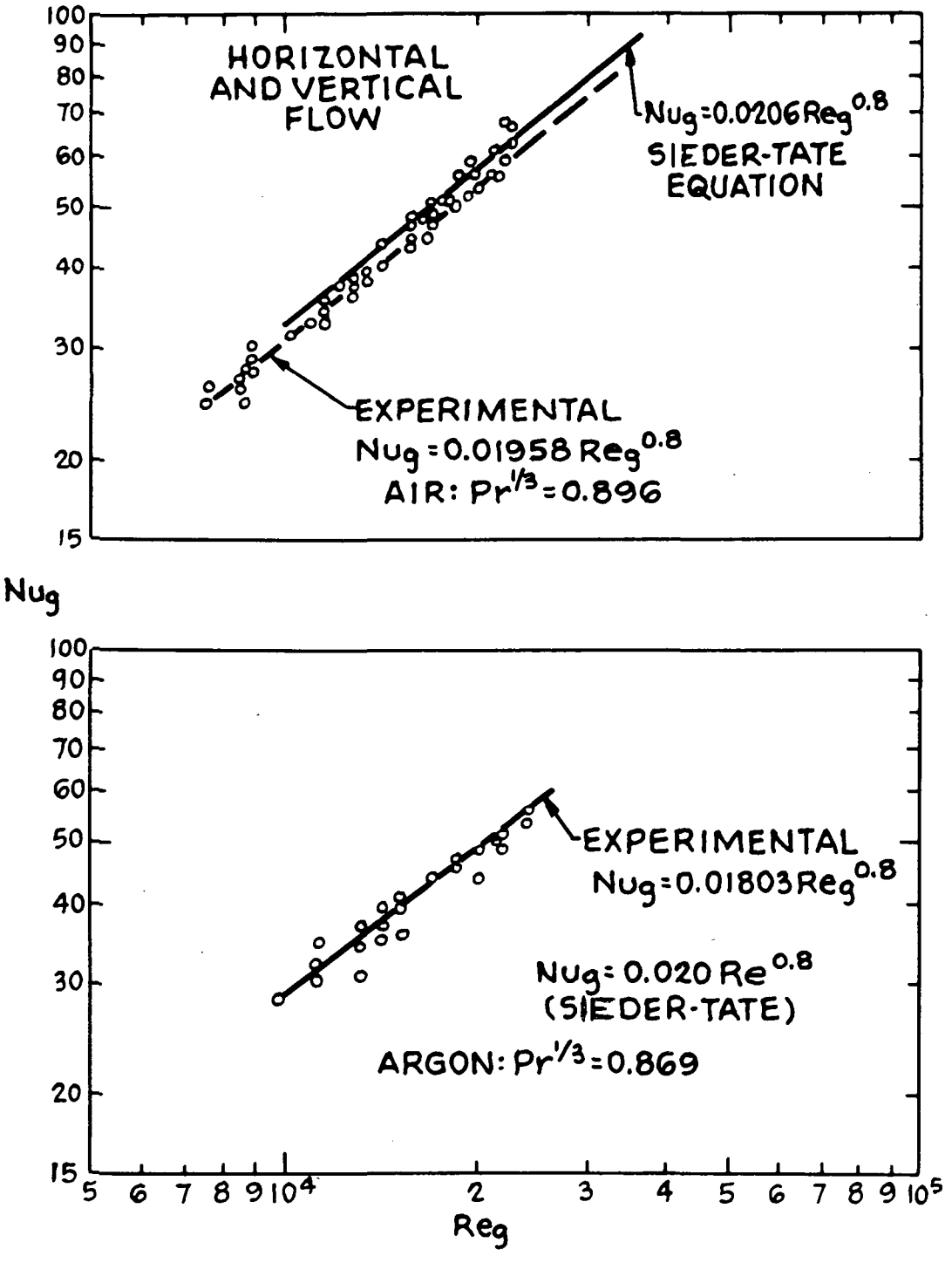

Figure 2 Clean Gas Nusselt Number Versus Reynolds Number

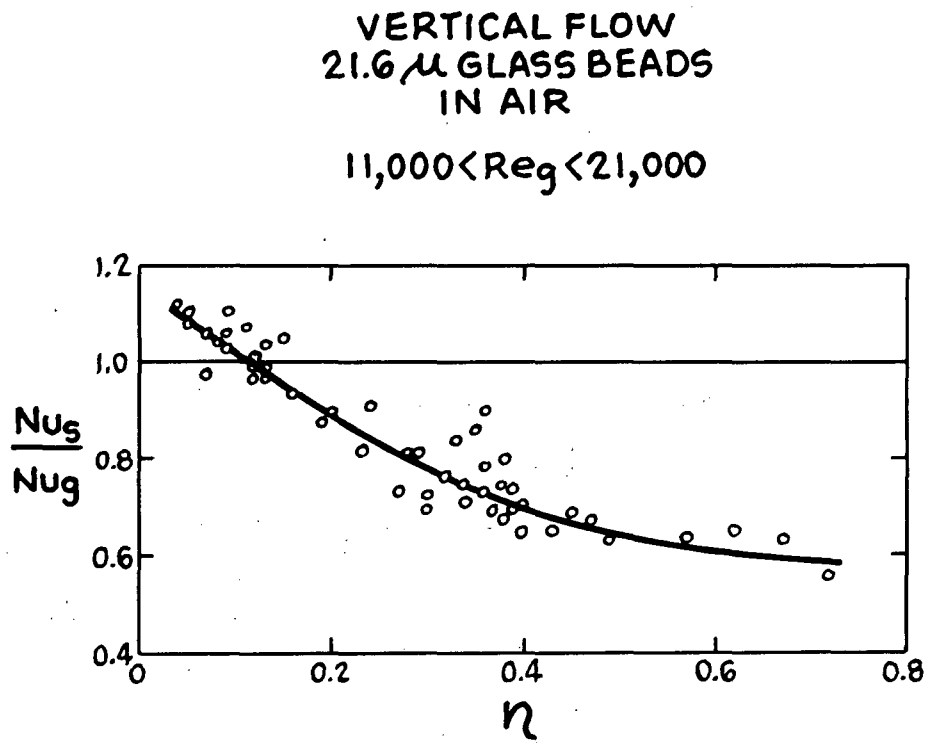

Figure 3 Vertical Nusselt Number Ratio Versus Loading Ratio - 21.6 Micron Glass Beads

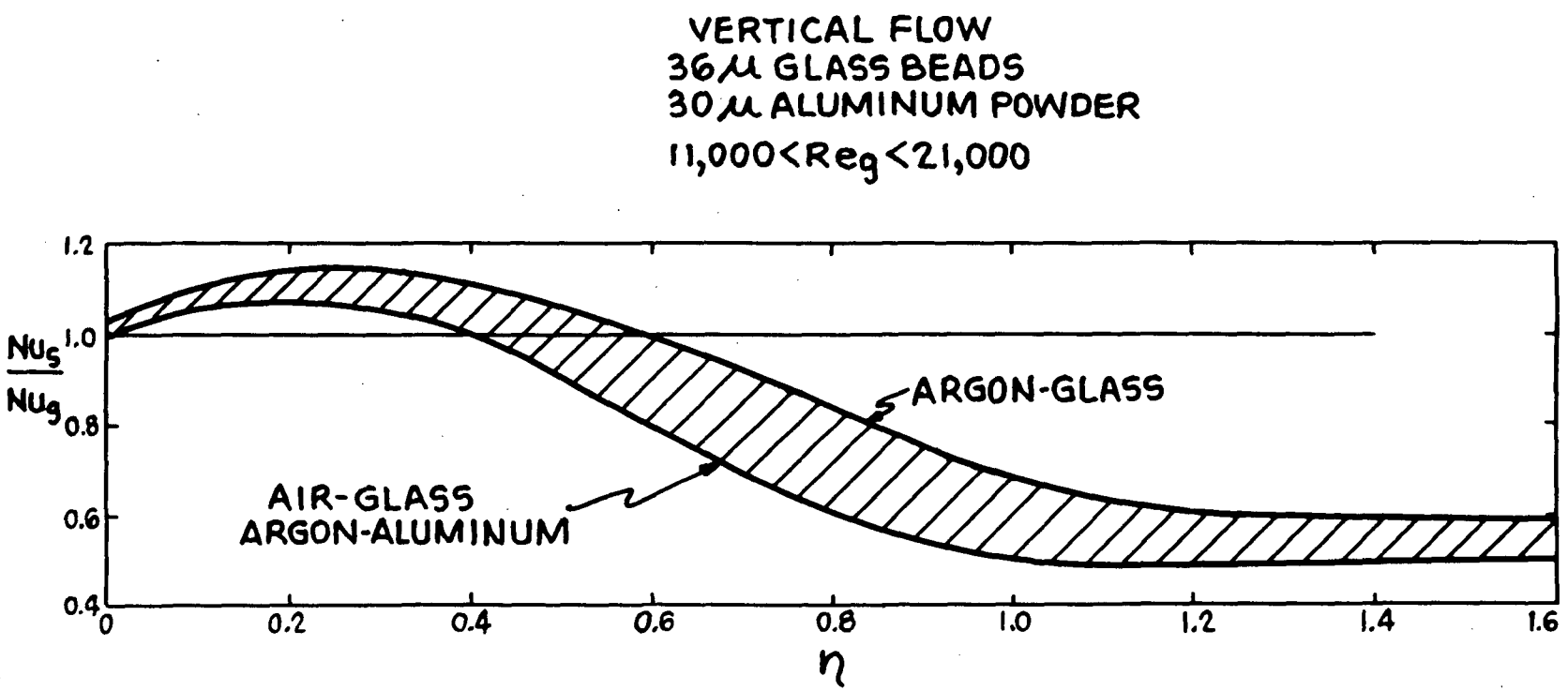

Figure 4 Vertical Nusselt Number Ratio Versus Loading Ratio - 36.0 Micron Glass Beads and 30.0 Micron Aluminum Powder

Figure 5 Horizontal Nusselt Number Ratio Versus Loading Ratio - 21.6 Micron Glass Beads

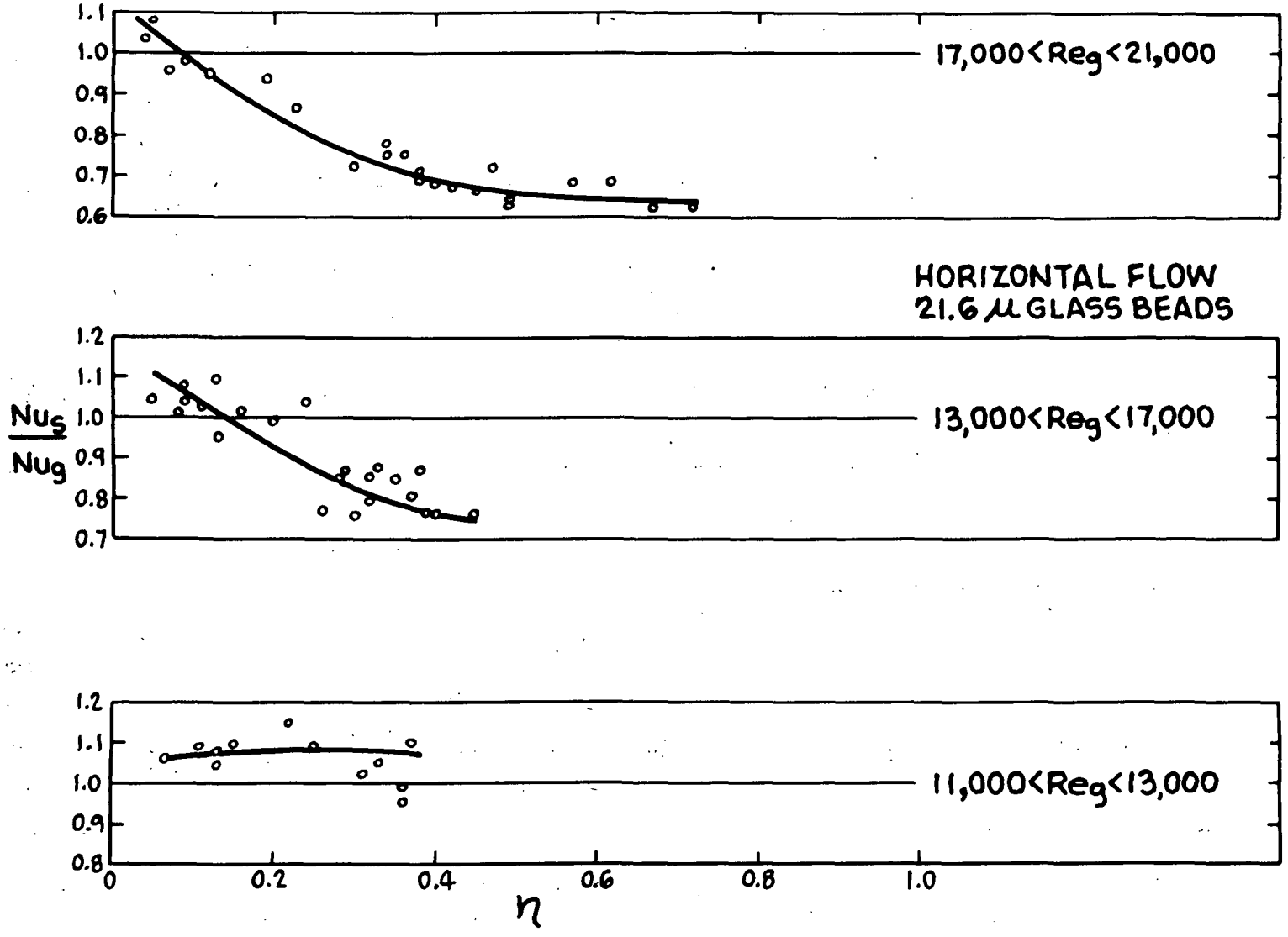

Figure 6 Horizontal Nusselt Number Ratio Versus Loading Ratio - 36.0 Micron Glass Beads and 30.0 Micron Aluminum Powder

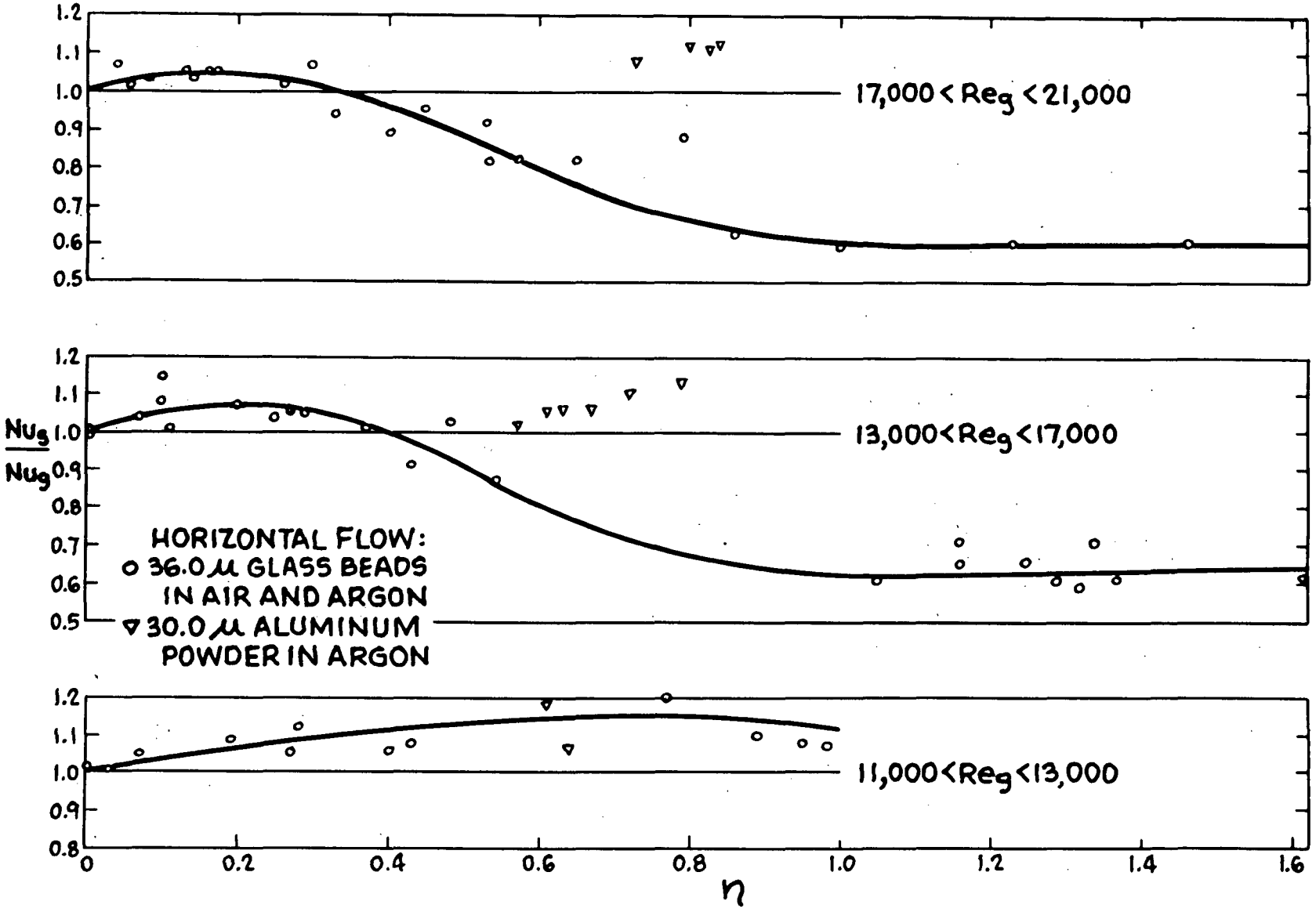

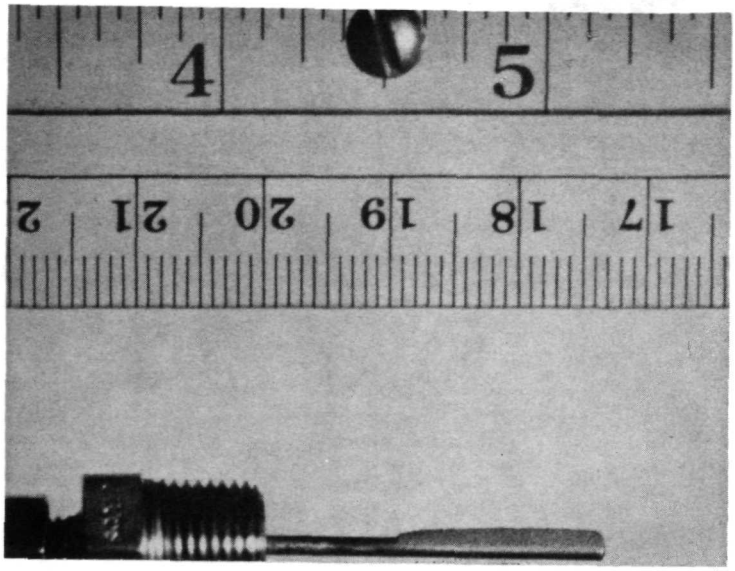

Figure 7

Aluminum Deposit on a Thermocouple

NASA-Langley, 1973 —— 33 E-7409

"The aeronautical and space activities of the United States shall be conducted so as to contribute . . . to the expansion of human knowledge of phenomena in the atmosphere and space. The Administration shall provide for the widest practicable and appropriate dissemination of information concerning its activities and the results thereof."

—NATIONAL AERONAUTICS AND SPACE ACT OF 1958

NASA SCIENTIFIC AND TECHNICAL PUBLICATIONS

TECHNICAL REPORTS: Scientific and technical information considered important, complete, and a lasting contribution to existing knowledge.

TECHNICAL NOTES: Information less broad in scope but nevertheless of importance as a contribution to existing knowledge.

TECHNICAL MEMORANDUMS: Information receiving limited distribution because of preliminary data, security classification, or other reasons. Also includes conference proceedings with either limited or unlimited distribution.

CONTRACTOR REPORTS: Scientific and technical information generated under a NASA contract or grant and considered an important contribution to existing knowledge.

TECHNICAL TRANSLATIONS: Information published in a foreign language considered to merit NASA distribution in English.

SPECIAL PUBLICATIONS: Information derived from or of value to NASA activities. Publications include final reports of major projects, monographs, data compilations, handbooks, sourcebooks, and special bibliographies.

TECHNOLOGY UTILIZATION PUBLICATIONS: Information on technology used by NASA that may be of particular interest in commercial and other non-aerospace applications. Publications include Tech Briefs, Technology Utilization Reports and Technology Surveys.

Details on the availability of these publications may be obtained from:

SCIENTIFIC AND TECHNICAL INFORMATION OFFICE

NATIONAL AERONAUTICS AND SPACE ADMINISTRATION

Washington, D.C. 20546